

SURFACE SOLAR RADIATION IN A TROPICAL AREA ESTIMATED FROM DIFFERENT MODELS

PAVÃO, Vagner Marques – vagnermpavao@gmail.com
Universidade Federal de Mato Grosso / UFMT

BIUDES, Marcelo Sacardi – marcelo@fisica.ufmt.br
Universidade Federal de Mato Grosso / UFMT

QUERINO, Carlos Alexandre Santos – carlosquerino@ufam.edu.br
Universidade Federal do Amazonas / UFAM

MACHADO, Nadja Gomes – nadja.machado@blv.ifmt.edu.br
Instituto Federal de Mato Grosso / IFMT

PAVÃO, Larissa Leite – lari_o.l@hotmail.com
Universidade Federal de Mato Grosso / UFMT

SILVA, Pablinne Cynthia Batista da Silva e – pablinne.cynthia06@gmail.com
Universidade Federal de Mato Grosso / UFMT

ABSTRACT: The Global Solar Radiation (R_g) is considered the main power that regulates the biophysical processes in the surface-atmosphere interface. Many regions of the Earth do not have those kinds of measures available, consequently approach models that allow confident estimates are necessary. Thus, the objective of this article was to evaluate the performance of the models proposed by Angström-Prescott (1940), Hay (1979) and Bristow & Campbell (1984) to estimate the solar global radiation in the city of Sinop, Mato Grosso state. Therefore, data from the National Institute of Meteorology (INMET), from 2006 to 2012, have been used to validate and parameterize the models. Solar Global Radiation (R_g), air temperature (maxima and minima), clarity atmospheric index (kt) and the relative sunshine duration (I_r) have shown seasonality under influence of the cloudiness. The R_g estimates for the models did not differ significantly from the R_g measurements and all the models showed a Pearson's correlation coefficient classified as "strong", except for those estimated by the Bristow & Campbell's model. However, the Hay's model presented smaller errors and higher coefficients of correlation and accuracy than the other models. The results indicate that all the models are applicable to the region, but additional surveys with other models covering all of Mato Grosso are necessary to improve the adjustment of the R_g estimation models

KEYWORDS: solar radiation modelling, sunshine duration, inter-comparison modelling.

RADIAÇÃO SOLAR DE SUPERFÍCIE EM UMA ÁREA TROPICAL ESTIMADA POR DIFERENTES MODELOS

RESUMO: A Radiação Solar Global (R_g) é considerada a principal fonte energética que regula os processos biofísicos na interface superfície-atmosfera. Muitas regiões da Terra não têm esses tipos de medidas disponíveis e, conseqüentemente, o ajuste de modelos que permitem estimativas confiantes são necessárias. Assim, o objetivo deste artigo foi avaliar o desempenho dos modelos propostos por Angström-Prescott (1940), Hay (1979) e Bristow & Campbell (1984) para estimar a radiação solar global na cidade de Sinop, Mato Grosso. Foram utilizados dados do Instituto Nacional de Meteorologia (INMET), de 2006 a 2012, para validar e parametrizar os modelos. A Radiação Solar Global (R_g), a temperatura do ar (máximos e mínimos), o índice de claridade atmosférico (kt) e a duração relativa do brilho solar (I_r) mostraram sazonalidade sob influência da

nebulosidade. As estimativas de R_g pelos modelos não diferiram significativamente das medidas de R_g e todos os modelos apresentaram coeficiente de correlação de Pearson classificado como "forte", exceto para aqueles estimados pelo modelo de Bristow & Campbell. No entanto, o modelo de Hay apresentou menores erros e maiores coeficientes de correlação e exatidão que os demais modelos. Os resultados indicam que todos os modelos são aplicáveis à região, mas pesquisas adicionais com outros modelos e abrangendo todo Mato Grosso são necessárias para melhorar o ajuste dos modelos de estimativa de R_g .

PALAVRAS-CHAVE: Precipitation, IAC, ODP, ENOS, Mundaú

1. INTRODUCTION

Brazil is one of the biggest grain producers of the world with annual production estimated in about 207 millions of tons throughout the 2014/2016 crop. Among all Brazilian states that produce grains, Mato Grosso comes as the second biggest agricultural producer, which represents 24% of the entire Brazilian production (CONAB 2014, 2016). The available region to produce grains in Mato Grosso covers about 8% of the total area of the state, mainly the cities of Sapezal, Campo Novo do Parecis, Nova Mutum, Primavera do Leste and Sinop (IBGE 2015).

The municipality of Sinop was created from the colonization processes of the Amazonia and Central-Northern region of Brazil throughout 1970 decade and was fostered by the Programa de Integração Nacional – PIN (National Integration Program) of the federal government (BOTELHO and SECCHI, 2014). This program had as main purpose to give support to immigrants who were looking for fertilized lands and economic prosperity. Sinop gained view in the regional context from the moment its population increased and the social-economical investments diversified through the agriculture expansion (BOTELHO and SECCHI, 2014). However, the agricultural expansion has been related to the intense deforestation that causes many regional climate impacts (SHEIL and MURDIYARSO, 2009), such as alteration on the energy balance pattern, evapotranspiration reduction, increasing of the surface albedo and temperature, and reduction of the surface roughness (BIUDES et al., 2015).

Solar radiation is the main font of energy to all energetic fluxes in the soil-plant-atmosphere system (BORGES et al., 2011). All kind of radiation originated from the Sun that reaches the Earth surface is called global solar radiation (R_g) (QUERINO et al., 2006). The knowledge of R_g and its components is crucial to understand the total available energy into the soil-plant-atmosphere system, and consequently, how the physical, chemical and biological processes, such as photosynthesis and thunderstorm development, happen in the surface-atmosphere interface (SOUZA et al., 2005; QUERINO et al., 2011).

The amount of R_g data available is limited, once there is a low number of weather stations that register this variable due to the high cost and frequently maintenance of the sensors (THORNTON and RUNNING, 1999; WEISS et al., 2001). Therefore, many math models have been suggested mainly based on empiric relation to estimate R_g by using meteorological variable such as relative humidity (YANG and KOIKE, 2002), rainfall (LIU and SCOTT 2001; RIVINGTON et al., 2005), sunshine fraction (TRNKA et al., 2005; CHEN et al., 2006), satellite data (MEHARRAR and BACHARI, 2014) and others. Among the models to estimate R_g , Angström-Prescott (1940) and Hay (1979), both based on the sunshine duration (n), show up as the most popular. The R_g estimated by these

models are driven from the coefficients a and b , which are determined by using linear regression between the atmospheric clearness index (k_t) and the relative sunshine duration. Nevertheless, Hay's model is different from Angström-Preussner's because it considers the surface reflection factor in its structure. The Bristow and Campbell's model (BRISTOW and CAMPBELL, 1984) assumes that the incoming solar radiation is a function of the local thermal amplitude, as well as of the solar radiation on the top of the atmosphere (R_0).

There are many models to estimate R_g but most of the studies use two types; temperature-based and sunshine-based models. The most famous sunshine-based model is Angström-Preussner's (LI et al., 2013). This model is commonly used because it suggests a linear relationship between the ratio of average daily R_g and sunshine ratio (DUZEN and AYDIN, 2012). According to the same authors, Angström-Preussner's performs better than temperature-based or cloud-based, because those last ones must to be calibrated to local parameters rather than others model. However, the limitations of those models are due to the simplifying assumption applied by them (MEHARRAR and BACHARI, 2014).

The estimation of the R_g varies according to each period of the year, which modifies the complexity of the estimation and the adjusting coefficients to reach the best result (BURIOL et al., 2012). Therefore, due to the importance of the agriculture potential of the Sinop city as well as the necessity of understanding the global solar radiation on the region, it is necessary to find alternative ways to estimate R_g . Thus, the objective of this paper was to evaluate the performance of Angström-Preussner (1940), Hay (1979) and Bristow and Campbell's (1984) models, and to adjust their respective coefficients, to estimate R_g in Sinop, MT.

2. MATERIAL AND METHODS

2.1. STUDY AREA

The study was carried out on the municipality of Sinop (Figure 1), which is located in the Central-Northern region of the Mato Grosso state on the margin of the Cuiabá – Santarém highway (BR 163). The site is placed under coordinates 12°07'53" S and 55°35'57" W and is 500 km far away from Cuiabá (capital city of Mato Grosso state). With a total area of 3.942.231 km² and an estimated population of about 126.000 inhabitants, Sinop is considered the biggest urban center of the Northern region of Mato Grosso state (IBGE, 2015).

The climatic condition of the city is hot and humidity with averaged annual temperature around 24°C. The rainfall pattern is equatorial which is characterized by a dry period throughout the austral winter and a wet season during the summer. The annual amount of rainfall is about 2091.6 mm year⁻¹ and the highest precipitation happens during the months of January, February and March, while the lowest amount of rainfall is observed in June, July and August (BIUDES et al., 2014).

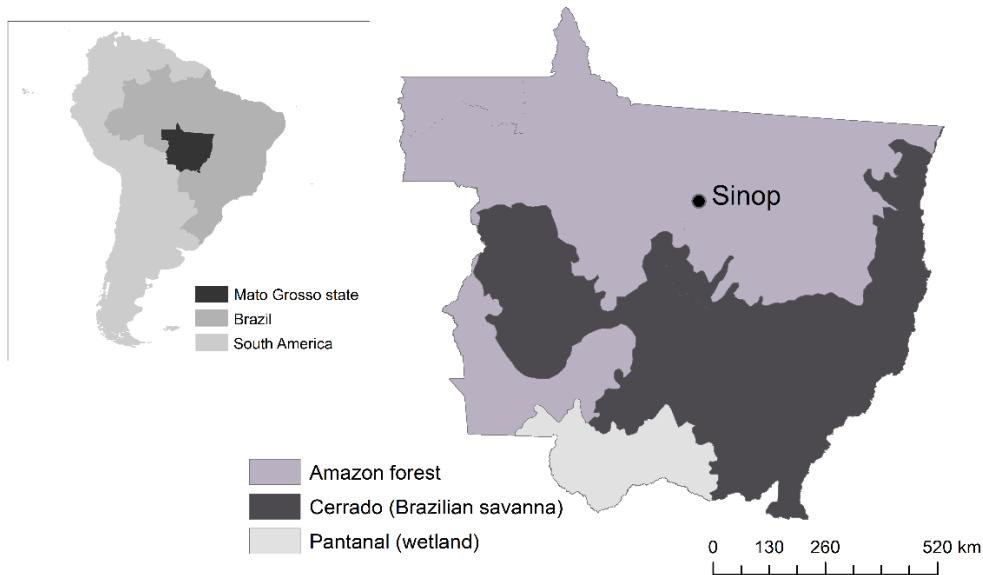


Figure 1 - Location map of the municipality of Sinop, Mato Grosso, Brazil.

2.2. ACQUIREMENT AND TREATMENT OF DATA

The data were acquired from the National Institute of Meteorology (INMET) between 2006 and 2012. The sunshine duration (n) was measured by a heliograph installed in a weather station placed in an occupation area near Sinop denominated Gleba Celeste (12.00°S and 56.50°W). The global solar radiation (R_g) was measured by the pyranometer LI200SA (LI-COR, Inc) mounted in the automatic weather station of the Sinop under coordinates 11.98°S and 55.57°W . To ensure the quality of the data processes, all negative values of R_g or higher than solar constant were eliminated.

2.3. ESTIMATIVE MODELS OF THE GLOBAL SOLAR RADIATION

Due to the absence of historical solar radiation data in Brazil, especially in the central and northern regions, three models were parameterized: two sunshine-based models and a temperature-based model. The choice of these models considered the most common data available on Brazilian meteorological stations, as well as the simplicity and precision of the models.

2.3.1. ANGSTRÖM-PRESCOTT'S MODEL

The Angström-PreScott's equation estimates R_g from the relative sunshine duration (I_r) and from the solar radiation on the top of the atmosphere (Equation 1) (DORNELAS et al., 2006).

$$R_g = R_o \left[a + b \left(\frac{n}{N} \right) \right] \quad (1)$$

where R_g is the daily global solar radiation in ($\text{MJ m}^{-2} \text{d}^{-1}$), n is the effective number of hours that the solar disc was exposed throughout the day (h)

d^{-1}) (sunshine duration), N is the potential sunshine duration ($h d^{-1}$) determined by the Equation (2), a and b are the linear and the angular coefficients respectively and R_o is the solar radiation incident on the top of the atmosphere ($MJ m^{-2} d^{-1}$) estimated by Equation (5).

$$N = \frac{2hp}{15} \quad (2)$$

where hp is the hourly angle to the sunset (Equation 3), calculated from the local latitude (φ) and from the solar declination (δ) (Equation 4).

$$hp = \cos^{-1}(-\tan \varphi \tan \delta) \quad (3)$$

$$\delta = 23.45 \sin \left[\frac{360(JD + 284)}{365} \right] \quad (4)$$

$$R_o = 37.6 dr(\sin \varphi \sin \delta + \cos \varphi \cos \delta \sin hp) \quad (5)$$

Julian day for JD and dr is the correction of the orbit eccentricity of the Earth (Equation 6).

$$dr = 1 + 0.033 \cos \left(\frac{360 JD}{365} \right) \quad (6)$$

2.3.2. HAY'S MODEL

The Hay's model is given by the Equation (7), and estimates R_g from the R_o , from the isolation rates, and also considers the multiple reflections of the atmosphere.

$$R_g = \frac{R_o}{A} \left[a' + b' \left(\frac{n}{N} \right) \right] \quad (7)$$

where a' and b' are linear and angular coefficients respectively, and A is the adjustment factor associated to the multiple reflections (Equation 8).

$$A = 1 - \alpha \left[\beta \frac{n}{N'} + \alpha_c \left(1 - \frac{n}{N'} \right) \right] \quad (8)$$

where α is the albedo of the grass (0.20) defined by the World Meteorological Organization (WMO) as the standard surface where a weather station should be installed. α_c is the albedo of the cloud bases, usually equals to 0.60, β the scattering coefficient of a clear atmosphere (0.25), N' is the potential sunshine duration for a specific day, and in this case, considering that the heliograph only registers when the Sun high is upper than 5° (Brooks and Brooks 1947), is estimated by Equation (9).

$$N' = \frac{2 \cos^{-1} \left(\frac{\cos 85^\circ - \sin \varphi \sin \delta}{\cos \varphi \cos \delta} \right)}{\pi} \quad (9)$$

2.3.3. BRISTOW AND CAMPBELL'S MODEL

The Bristow and Campbell's Model estimates the daily global solar radiation (R_g , MJ m⁻² d⁻¹) as function of the daily solar radiation incident on the top of the Earth atmosphere (R_o , MJ m⁻² d⁻¹) and also as function of the daily thermal amplitude, which is the difference between the maximum and minimum register of the daily temperature (ΔT , °C) (Equation 10).

$$R_g = R_o A \left[1 - e^{(B\Delta T^C)} \right] \quad (10)$$

The empiric constants A, B and C have a physical meaning, once that the A coefficient represents the maxima expected solar radiation for a certain day under clear sky condition and B and C control the variations of A when increasing of the temperature difference happen. The original values of the coefficients are A = 0.7, B = between 0.004 and 0.010, and C=2.4 (QUEIROZ et al., 2000). The Bristow-Campbell's model was parameterized by using daily values and we expect that new values of the coefficients can be obtained with the application of the model by using the monthly data.

2.4. ATMOSPHERIC CLEARNESS INDEX (KT) AND ISOLATION RATES (IR)

The Atmospheric Clearness Index (kt) is the ratio between R_g and R_o (Equation 11) (RENSHENG et al., 2004). The relative sunshine duration (Ir) is the ratio between sunshine duration (n) and potential sunshine duration (N) (Equation 12).

$$Kt = \frac{R_g}{R_o} \quad (11)$$

$$Ir = \frac{n}{N} \quad (12)$$

2.5. STATISTICS ANALYSIS

The monthly, seasonal and annual averages in a confident interval of ± 95% of the meteorological variables and measured and estimated R_g have been calculated by the 1000 iteration of the bootstrapping of the aleatory resampling with substitution (EFRON e TIBSHIRANI, 1993). The values of R_g estimated by the models were confronted with R_g measured in the weather station by Wilmott's accordance index d (Equation 13) (WILLMOTT et al., 1985), Pearson's correlation coefficient r (Equation 14), the Root Mean Square Error (RMSE) (Equation 15) and the Mean Absolute Error (MAE) (Equation 16).

$$d = 1 - \frac{\sum_{i=1}^n (P_i - O_i)^2}{\sum_{i=1}^n (|P_i - O| + |O_i - O|)^2} \quad (13)$$

$$r = \frac{\sum_{i=1}^n (P_i - P)(O_i - O)}{\sqrt{\sum_{i=1}^n (P_i - P)^2 \sum_{i=1}^n (O_i - O)^2}} \quad (14)$$

$$RMSE = \sqrt{\frac{\sum_{i=1}^n (P_i - O_i)^2}{n}} \tag{15}$$

$$MAE = \frac{\sum_{i=1}^n |P_i - O_i|}{n} \tag{16}$$

where P_i are the estimated values of Rg , P is the averaged value of the estimated Rg , O_i is the value of the measured Rg , O is the averaged value of the measured Rg and n is the number of observations. The Willmott's index shows its results based on different levels of performance established on the distance between the estimated and measured values. Its value varies from 0 (no accordance) to 1 (perfect accordance). The Pearson's correlation coefficient indicates a measure of the level and the signal of the correlation between two variables and it is placed from -1 to 1. The $MSRE$ shows the fail of the model when it estimates variability of the measurement related to the average and gives the variation of the values estimated by the measured values, and the MAE indicates the absolute distance (deviation) of the averages. The minimum limit of the $MSRE$ and of the MAE is 0, which represents a perfect approach between the real data and the model's estimative. The index proposed by Devore (2006) (Table 1) has been used to classify the correlation between measured Rg and the one estimated by the models.

Table 1 - Classification of the Pearson's correlation coefficient (r) to the Rg estimative methods (DEVORE, 2006).

r	Definition
0,00 a 0,19	Extremely weak correlation
0,20 a 0,39	Weak Correlation
0,40 a 0,69	Moderate correlation
0,70 a 0,89	Strong correlation
0,90 a 1,00	Extremely strong correlation

3. RESULTS AND DISCUSSION

3.1. ANALYSIS OF THE METEOROLOGICAL VARIABLES

The major accumulation of precipitation happened during the seven months of the wet season (October to April) which corresponds to 95% of the annual total amount of the rain, meanwhile the lowest register of rainfall was observed during the five months of the dry season (May to September) equivalent to 5% of the annual total (Table 2 and Figure 2a). The month with the highest sum of rainfall was January, corresponding to 19% of the total precipitation while lowest was registered in July, corroborating to Biudes et al., (2012; 2015). The rainfall regime on the study region is governed mainly by large-scale phenomenon such as the acting of the Bolivia high pressure and South Atlantic Convergence Zone (SACZ). The SACZ is characterized by a huge nebulosity cover that extends from the South of Amazon to the Southeast of Brazil, influencing on the amount of rainfall in the Central-Western region (ESCOBAR, 2014). The Bolivia high pressure acts during the summer and

creates a meridional flow that helps to create instability zones in the central area of the country, inducing the rain formation (VIANELLO and MAIA, 1986; CARVALHO and JONES, 2009). The non-actuation of these phenomena, throughout the winter season, results in the lowest amount of rainfall on the study area (ESCOBAR, 2014).

Table 2 - Monthly, seasonal and annual total of the precipitation and average (\pm 95% confidence interval) of the solar radiation on the top of the atmosphere (R_o ; $MJ\ m^{-2}\ d^{-1}$), of the global solar radiation (R_g ; $MJ\ m^{-2}\ d^{-1}$), averaged (T_{avg} ; $^{\circ}C$), maximum (T_{max} ; $^{\circ}C$), and minimum temperature (T_{min} ; $^{\circ}C$), atmospheric clearness index (K_t) and isolation rates (Ir) between the year of 2006 and 2012 in Sinop, Mato Grosso, Brazil

Month	Ppt	Ro	Rg	Tavg	Tmax	Tmin	Kt	Ir
Jan	376.8	40.1 \pm 0.0	19.4 \pm 0.8 4	24.4 \pm 0.1 6	29.9 \pm 0.2 7	21.4 \pm 0.1 1	0.49 \pm 0.0 2	0.39 \pm 0.03
Feb	343.2	39.5 \pm 0.1	20.0 \pm 0.7 5	24.7 \pm 0.1 8	30.6 \pm 0.3 6	21.4 \pm 0.1 3	0.51 \pm 0.0 2	0.41 \pm 0.03
Mar	197.3	37.4 \pm 0.2	19.9 \pm 0.7 6	25.1 \pm 0.1 7	31.3 \pm 0.2 5	21.5 \pm 0.1 1	0.53 \pm 0.0 2	0.47 \pm 0.03
Apr	156.2	33.8 \pm 0.2	18.7 \pm 0.6 6	25.3 \pm 0.1 9	31.5 \pm 0.2 8	21.1 \pm 0.1 6	0.55 \pm 0.0 2	0.56 \pm 0.03
May	29.3	30.1 \pm 0.1	18.6 \pm 0.4 6	25.2 \pm 0.3 8	31.7 \pm 0.3 4	19.9 \pm 0.4 9	0.62 \pm 0.0 1	0.67 \pm 0.03
Jun	11.2	28.2 \pm 0.0	18.4 \pm 0.3 0	25.6 \pm 0.4 0	32.9 \pm 0.2 7	19.0 \pm 0.6 1	0.65 \pm 0.0 1	0.77 \pm 0.02
Jul	5.4	29.1 \pm 0.2	19.2 \pm 0.3 7	26.0 \pm 0.4 5	33.6 \pm 0.2 5	18.3 \pm 0.6 5	0.66 \pm 0.0 1	0.79 \pm 0.02
Aug	6.8	32.4 \pm 0.2	20.3 \pm 0.3 5	26.6 \pm 0.3 7	35.0 \pm 0.2 7	17.9 \pm 0.5 8	0.63 \pm 0.0 1	0.75 \pm 0.02
Sep	39.8	36.1 \pm 0.2	19.9 \pm 0.5 4	27.4 \pm 0.3 1	35.6 \pm 0.4 1	19.8 \pm 0.3 1	0.55 \pm 0.0 2	0.58 \pm 0.04
Oct	204.7	38.7 \pm 0.1	20.3 \pm 0.6 6	26.2 \pm 0.2 2	33.2 \pm 0.4 0	21.4 \pm 0.1 7	0.52 \pm 0.0 2	0.48 \pm 0.03
Nov	329.1	39.7 \pm 0.0	20.1 \pm 0.7 2	25.3 \pm 0.1 7	31.4 \pm 0.3 2	21.6 \pm 0.1 1	0.51 \pm 0.0 2	0.42 \pm 0.03
Dec	361.7	40.0 \pm 0.0	19.0 \pm 0.7 8	24.5 \pm 0.1 5	30.0 \pm 0.2 8	21.4 \pm 0.1 2	0.48 \pm 0.0 2	0.37 \pm 0.03
Wet	1969.0	38.5 \pm 0.1	19.6 \pm 0.7 4	25.1 \pm 0.1 8	31.1 \pm 0.3 1	21.4 \pm 0.1 3	0.51 \pm 0.0 2	0.44 \pm 0.03
Dry	92.5	31.2 \pm 0.1	19.2 \pm 0.4 0	26.2 \pm 0.3 8	33.8 \pm 0.3 1	19.0 \pm 0.5 3	0.62 \pm 0.0 1	0.71 \pm 0.03
Annual	2061.6	35.4 \pm 0.1	19.5 \pm 0.6 0	25.5 \pm 0.2 6	32.2 \pm 0.3 1	20.4 \pm 0.3 0	0.56 \pm 0.0 2	0.56 \pm 0.03

The maximum R_o has happened in January and the lowest in July (Table 2 and Figure 2b). The interval with the lowest monthly average of R_o was from April to August and the highest averages from September to March. These intervals, respectively, correspond to the period that the Sun, on its apparently position, is located in the North Hemisphere (autumn and winter) and South Hemisphere (spring and summer), then, lower and higher solar radiation will occur on the top of the atmosphere (DALLACORT et al., 2004).

In a general, R_g has shown less accentuated variations when compared with the R_o 's temporal dynamic. The period of the maximum averaged of R_g was observed between October and April (rainy season), when the R_g was nearly 2% higher than the values registered between May and September (dry season) (Table 2 and Figure 2d). Nevertheless, the maximum monthly averaged

of Rg was noticed in August (dry season) when the cloud cover is lower in the region (BIUDES et al., 2015).

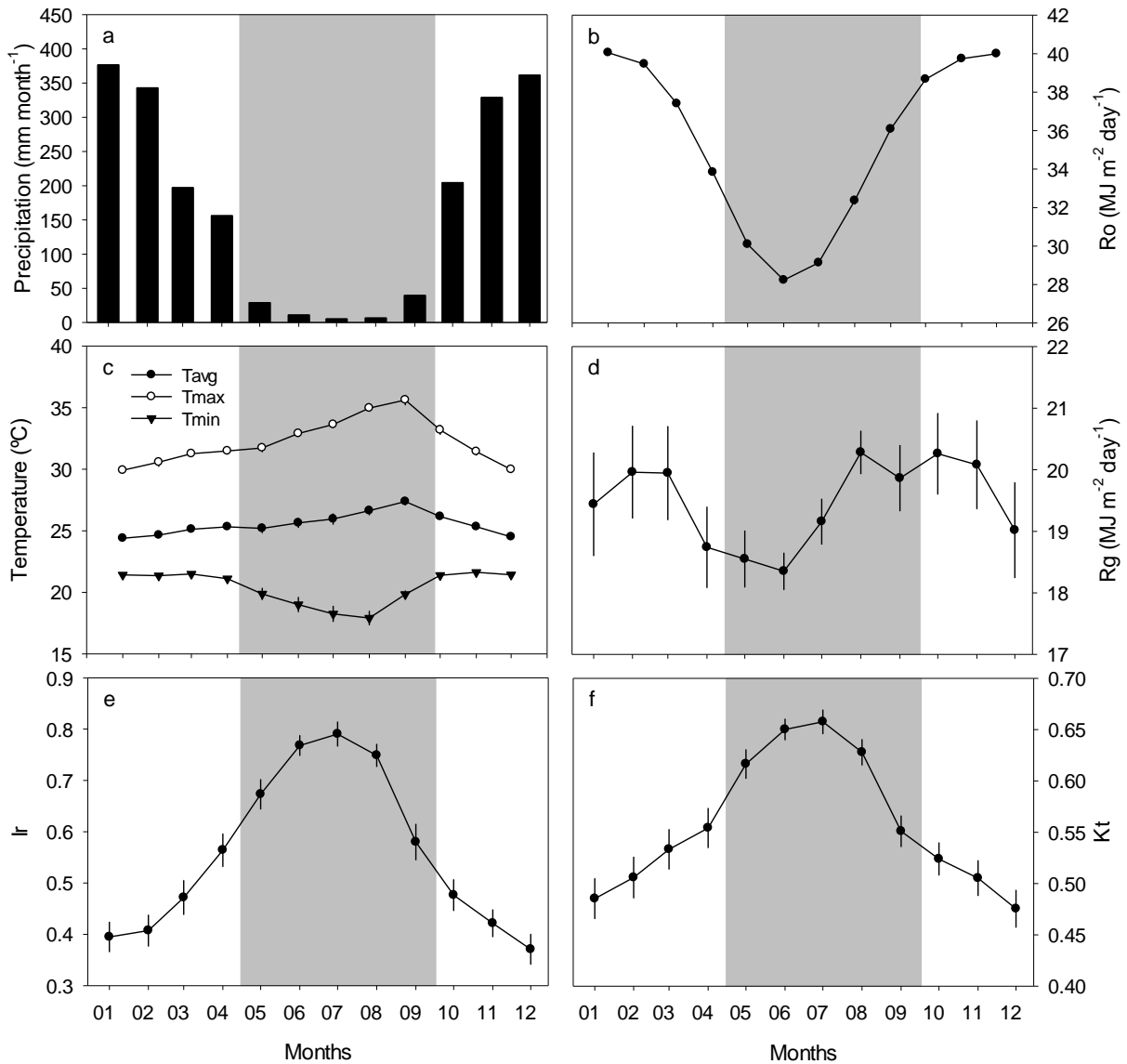


Figure 2 - Total precipitation (a), Solar Radiation on the top of the Atmosphere (Ro) (b), average, maxima and minima temperature of the air (c), Global Solar Radiation (Rg) (d), relative sunshine duration (Ir) (e) and Atmospheric Clearness Index (kt) (f) to the period from 2006 through 2012 in Sinop – MT.

The highest averages of Rg were observed in the wet season and are related with high intensity of Ro throughout that period. Thus, even though a reduction of Rg in function of the cloudiness during the rainy time is noticed, the intensity of Ro overcomes the averages values of Rg when compared to the dry period. Comparing values of Rg and Ro, it was observed a relation of 49% between Rg and Ro in January (maximum monthly average of Ro), and 65% in

June (minimum monthly average of R_o). These results suggest that the oscillation of R_g in Sinop does not depend only on the intensity of R_o , but also depends on the local atmospheric clearness (kt), which determines what is the portion of R_o that is attenuated by the atmosphere (QUERINO et al., 2011).

The mean air temperature during the study period oscillated between 24 and 27°C with values throughout the dry season 4% higher than the rainy period (Table 2 and Figure 2c). Between October and April (rainy season) it was observed the lowest variations among maxima and minima air temperature, with thermal amplitude varying from 8 to 12°C, and from May to September (dry period) the thermal amplitude oscillated from 12 to 17°C.

The lowest and uniform thermal amplitudes during the wet time are in function of the atmospheric moisture. The water acts as an air temperature moderated factor due to its elevated specific heating, inhibiting an abrupt increasing and decreasing of the air temperature. However, large daily amplitudes on the dry period happen due to the low quantity of clouds (and consequently water vapor) in the atmosphere. Despite of a high warming during the diurnal time, most of the infrared radiation, emitted by the surface, is rapidly released to the atmosphere and escapes to the space, causing cooling of the air during the nocturnal time. Another cause that can influence the thermal amplitude is the phenomenon called "friagens", common in the region and that normally generate significant decreasing in the air temperature (MARENGO and NOBRE, 2009; BIUDES et al., 2012).

The maximum value of I_r has happened in July and the minimum in December (Table 2 and figure 2e). The occurrence interval of the lowest values of I_r was in the period from October to April (rainy period) and the highest from May to September (dry period). The reason is probably because the sky presents less nebulosity (high insolation n) throughout the dry season, it presents also the lowest potential sunshine duration (N) (autumn and winter) and, consequently, I_r tends to be higher.

The kt has shown similar patterns of the I_r (Table 2 and Figure 2f) and its monthly maximum was in July while the minimum in December. That means a reduction of 28% of the incoming solar radiation reaching the surface when compared the months of maximum and minimum kt . The months with highest values of kt were concentrated from May to September, and the lowest from October to April, dry and wet seasons respectively.

We could observe an inversely proportional relation among the lowest values of kt with the months of high amount of precipitation, due to the major concentration of clouds during this period. The nebulosity, defined as the cloud cover in a certain place, acts as the main attenuation factor of the incoming solar radiation over surface (MENEZES and DANTAS, 2002). Another element that should be considered in our analysis is that during the rainy season, the sun is placed in the South Hemisphere, and consequently, highest values of R_o . Nevertheless, despite of biggest radiative fluxes on the top of the Earth atmosphere, just a small portion of the solar radiation will reach the surface, due to the concentration of clouds that tends to scatter the radiation, and reduce the atmospheric transmissivity (QUERINO et al., 2011).

3.2. APPLICATIONS OF THE MODELS

The lowest values of the coefficient *a* to the Angström-Prescott's model occurred in January, April and December, and the highest in July, and have shown smooth seasonal variations during the period (Table 3). On the other hand, the coefficient *b* has shown the highest values in December and the lowest in July with low seasonal variation. The *a* coefficient indicates a low *kt* in a day totally cloudy, what explain the occurrence of the lowest values of *a* in the rainy period (CAMPELO, 1998; DALLACORT et al., 2004). The sum of the coefficients *a* and *b* is related with the maximum *kt* when the *Ir* tends to 1. Hence, considering the annual coefficients to a total situation of nebulosity, it was verified for a *kt* equals to 0.32, with an *Ir* tending to 1, we obtain *kt* equals to 0.75.

The lowest values of *a* on the Hay's model happened in January, April and December, while the major ones were noticed in July (Table 3). The maximum coefficient *b* was observed in December and the lowest in July. The angular coefficients determined by Hay's equations are similar to that one obtained with Angström-Prescott's equation. This similarity is explained because of the results of the compensatory effect of the differences presented between these two models, where the introduction of the insolation rates that effectively can reach 1, would have the opposite effect to the insertion of parameters that consider the multiple reflection of the short wave (CAMPELO, 1998).

The *A* coefficient to the Bristow & Campbell's equation was fixed in all equations, varying only the coefficients *B* and *C* (Table 3). The lowest values of *B* happened in January, June, July, August and October, and the highest in May. The *C* coefficient has shown the lowest value in May and the highest in January.

Table 3 - Annual, Seasonal and Monthly coefficients (\pm confidence interval) to the Angstrom-Prescott, Hay and Bristow & Campbell models to Sinop - MT.

Period	Angström-Prescott			Hay			Bristow & Campbell			
	<i>a</i>	<i>b</i>	R ²	<i>a'</i>	<i>b'</i>	R ²	<i>A</i>	<i>B</i>	<i>C</i>	R ²
January	0.28±0.03	0.51±0.07	0.61	0.25±0.03	0.50±0.06	0.65	0.7	0.004	2.55	0.67
February	0.31±0.03	0.47±0.06	0.64	0.27±0.03	0.47±0.06	0.66	0.7	0.022	1.74	0.69
March	0.31±0.03	0.48±0.06	0.65	0.27±0.03	0.47±0.05	0.70	0.7	0.010	2.01	0.30
April	0.28±0.04	0.48±0.06	0.65	0.24±0.03	0.48±0.05	0.69	0.7	0.025	1.65	0.26
May	0.36±0.04	0.37±0.05	0.57	0.31±0.03	0.39±0.05	0.63	0.7	0.063	1.28	0.38
June	0.31±0.04	0.45±0.05	0.72	0.26±0.03	0.46±0.04	0.76	0.7	0.004	2.41	0.70
July	0.40±0.07	0.32±0.09	0.44	0.35±0.07	0.35±0.08	0.51	0.7	0.004	2.50	0.31
August	0.29±0.04	0.45±0.05	0.70	0.25±0.04	0.46±0.05	0.74	0.7	0.004	2.39	0.24
September	0.35±0.03	0.34±0.05	0.61	0.30±0.03	0.36±0.05	0.66	0.7	0.007	2.18	0.31
October	0.33±0.03	0.40±0.06	0.58	0.29±0.03	0.40±0.06	0.61	0.7	0.004	2.41	0.37
November	0.32±0.03	0.45±0.07	0.57	0.27±0.03	0.44±0.06	0.58	0.7	0.006	2.33	0.72
December	0.28±0.03	0.52±0.07	0.62	0.24±0.02	0.51±0.06	0.66	0.7	0.011	2.08	0.68
Dry Period	0.33±0.02	0.40±0.02	0.68	0.28±0.02	0.42±0.02	0.72	0.7	0.004	2.36	0.46
Wet Period	0.30±0.01	0.47±0.02	0.62	0.26±0.01	0.46±0.02	0.67	0.7	0.046	1.45	0.35
Annual	0.33±0.02	0.40±0.02	0.68	0.27±0.01	0.44±0.01	0.74	0.7	0.012	2.11	0.43

The R_g estimated by all models was not significantly different from the R_g measured in the study area, except the Bristow & Campbell model in the monthly and annual survey, which underestimated R_g by 3,1% and overestimated R_g by 5.5%, respectively (Table 4). The Angström-PreScott and Hay's models have presented good estimates to all study period (monthly, seasonal and annual), with accordance index (d) oscillating from 0.86 and 0.87, and correlation coefficient (r) varying between 0.76 and 0.79, and then, been classified as strong correlation (Figure 3 and Table 4).

The Bristow & Campbell's model had accordance index below 0.80 in the seasonal analysis and 0.83 in the annual and monthly investigations (Figure 3 and Table 4). The correlation coefficient was below 0.65 to the seasonal evaluations (moderated correlation) and has varied between 0.72 and 0.70 (strong correlation) in the annual and monthly comparisons respectively.

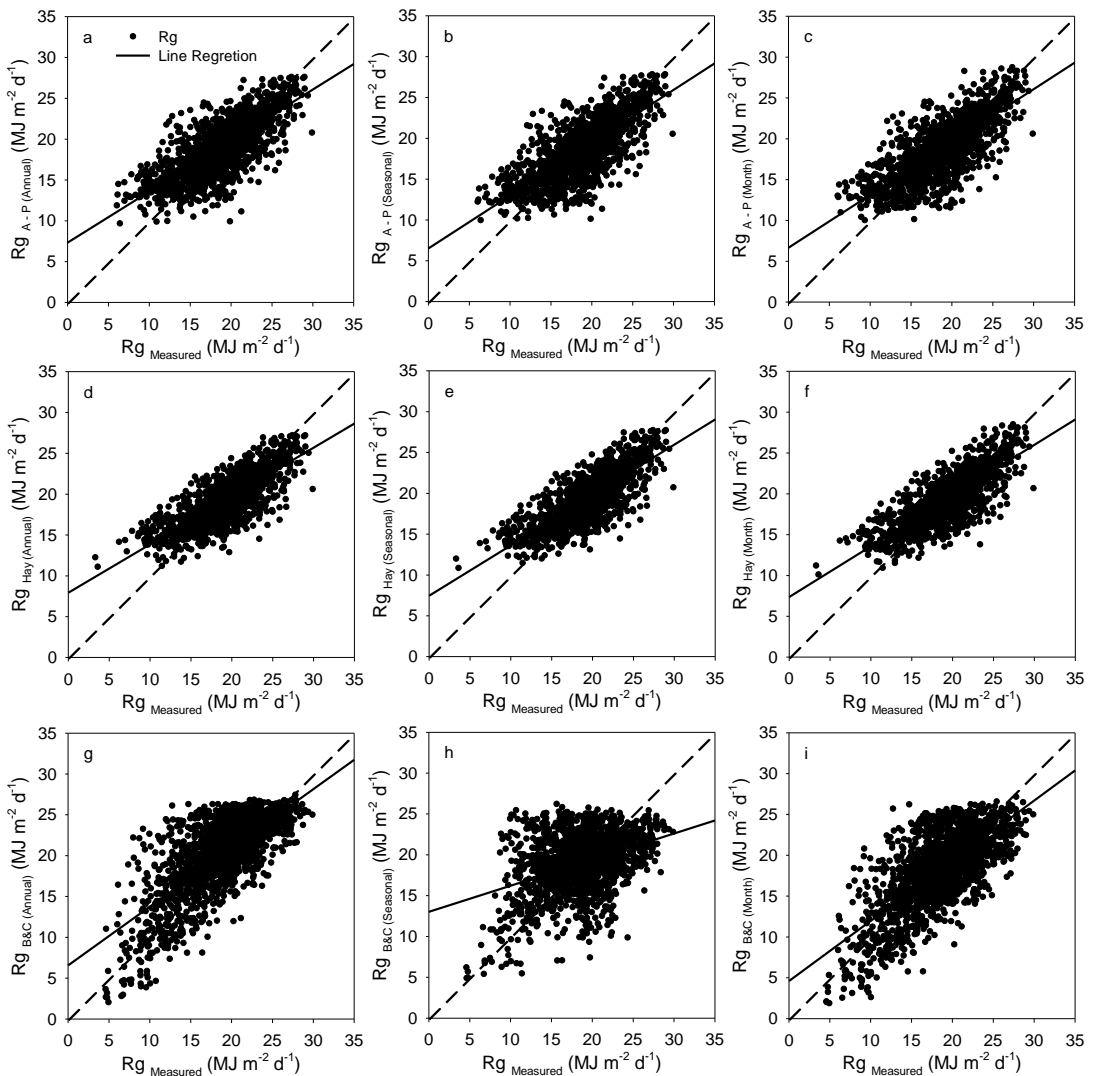


Figure 3 - Annual, seasonal and monthly relations between the R_g measured and estimated with the Angström-PreScott (a, b, c), Hay (d, e, f), and Bristow & Campbell's model (g, h, i).

Table 4 - Mean \pm CI (95% Confidence Interval), Root Mean Square Error (RMSE), Mean Absolute Error (MAE), Willmott's accordance index (*d*), Pearson's correlation coefficient (*r*) and intercept and slope of linear regression of estimated and measured solar radiation (*R_g*).

Models	Mean \pm CI	RMSE	<i>d</i>	MAE	<i>r</i>	Intercept	slope
Annual <i>R_g</i> (Measured)	19.66 \pm 0.20						
Annual <i>R_g</i> (Prescot)	19.77 \pm 0.16	2.67	0.86	1.99	0.76	7.32	0.63
Seasonal <i>R_g</i> (Prescot)	19.40 \pm 0.16	2.68	0.86	2.01	0.76	6.51	0.65
Monthly <i>R_g</i> (Prescot)	19.56 \pm 0.16	2.64	0.87	1.95	0.77	6.67	0.65
Annual <i>R_g</i> (Hay)	19.53 \pm 0.17	2.42	0.86	1.82	0.78	7.93	0.59
Seasonal <i>R_g</i> (Hay)	19.55 \pm 0.16	2.41	0.87	1.81	0.78	7.46	0.62
Monthly <i>R_g</i> (Hay)	19.56 \pm 0.17	2.38	0.87	1.77	0.79	7.37	0.62
Annual <i>R_g</i> (B e C)	20.74 \pm 0.19	3.47	0.83	2.56	0.72	6.55	0.72
Seasonal <i>R_g</i> (B e C)	19.44 \pm 0.17	3.88	0.77	2.72	0.64	9.89	0.49
Monthly <i>R_g</i> (B e C)	19.05 \pm 0.20	3.41	0.83	2.67	0.70	4.60	0.74

The difference presented by Bristow & Campbell's model and the other two models, especially during the winter, is associated to the thermal amplitude. The linear Angström-Prescott's model tend to be more accurate due to the established relationship between *R_g* and relative sunshine duration, and the need for calibration of local physical parameters (DUZEN AND AYDIN, 2012). The lower performance of the Bristow & Campbell model may be due to the model's inability to explain *R_g* variability and variation in daily thermal amplitude that was not significant over the study period (BELÚCIO et al., 2014).

4. CONCLUSIONS

The variables *R_g*, temperature (maxima and minima), *kt* and *Ir* have presented seasonality, mainly driven by the nebulosity.

Although the *R_g* estimates for the models did not differ significantly from the *R_g* measurements and that all models had Pearson's correlation coefficient classified as "strong", except for those estimated by the Bristow & Campbell's model. The Hay's model showed a better performance in relation to the other models studied. Probably, the best performance of the Hay's model was due to the insertion of the adjustment factor "A", which considers multiple reflections of *R_g* in the atmosphere.

Even though the *R_g* estimated by the Bristow & Campbell's model differed significantly from the *R_g* measured, on average that difference was around 5%. This means that in the absence of the measure of sunshine duration, the *R_g* of the study region can be also estimated by the Bristow & Campbell's model.

Our results suggest that further research should be carried out, such as application of the models to the other areas of the Mato Grosso state to improve the estimative *R_g* on the study region, as well as on the whole state.

5. ACKNOWLEDGMENTS

Research was partly funded by the Universidade Federal de Mato Grosso (UFMT), Instituto Federal de Mato Grosso (IFMT), Universidade Federal do Amazonas (UFAM), Instituto Nacional de Meteorologia (INMET), Coordenação de Aperfeiçoamento de Pessoal de Nível Superior (CAPES), Conselho Nacional de Desenvolvimento Científico e Tecnológico (CNPq) under grant number 303625/2015-5; 310879/2017-5; Edital Universal/CNPq - 407463/2016-0, Fundação de Amparo à Pesquisa do Estado de Mato Grosso, under grant FAPEMAT – PRONEM - 561397/2014.

6. REFERENCES

ANGSTROM, A. Solar and terrestrial radiation. *Quart J of Roy Meteor Soc*, London 50: 121-125, 1924.

ARAUJO, R.A.; COSTA, R.B.; FELFILI, J.M.; GONÇALVES, I.K.; SOUSA, R.A.T.M.; DORVAL, A. Florística e estrutura de fragmento florestal em área de transição na Amazônia Matogrossense no município de Sinop. *Act Amaz.* v.9(4), 865 – 878, 2009.

BELÚCIO, P.B.; DA SILVA, A.P.N.; SOUZA, L.R.; MOURA, G.B.A. Radiação solar global estimada a partir da insolação para Macapá (AP). *Rev Bras de Meteorol.* v. 29(4), 494-504, 2014.

BIUDES, M.S.; NOGUEIRA, J.S.; DALMAGRO, H.J; MACHADO, N.G.; DANELICHEN, V.H.M.; SOUZA, M.C. Mudança no microclima provocada pela conversão de uma floresta de cambará em pastagem no norte do Pantanal. *Rev de Ciên Agro-Amb.* v.10(1), 61-68, 2012.

BIUDES, M.S.; SOUZA, M.C.; MACHADO, N.G.; DANELICHEN, V.H.M.; VOURLITIS, G.L.; NOGUEIRA, J.S. Modelling gross primary production of a tropical semi-deciduous forest in the southern Amazon Basin. *Int J Remote Sens.* v.34(4), 1540–1562, 2014.

BIUDES, M.S.; VOURLITIS, G.L.; MACHADO, N.G.; ARRUDA, P.H.Z.; NEVES, G.A.R.; LOBO, F.A. NEALE, C.M.U; NOGUEIRA, J.S. Patterns of energy exchange for tropical ecosystems across a climate gradient in Mato Grosso, Brazil. *Agric and For Meteorol.* v.202, 112–124, 2015.

BORGES, V.P.; OLIVEIRA, A.S.; FILHO, M.A.C.; SILVA, T.S.M.; PAMPONET, B.M. Avaliação de modelos de estimativa da radiação solar incidente em Cruz das Almas, Bahia. *Rev Bras de Eng Agr e Amb.* v.14 (1), 74–80, 2010.

BOTELHO, M.T.S.L.; SECCHI, D. O processo de colonização em Mato Grosso e o impacto sobre as sociedades indígenas: o caso de Sinop. *Tellus.* v.26, 31 – 48, 2014.

BRISTOW, K.L.; CAMPBELL, G.S. On the relationship between incoming solar radiation and daily minimum and maximum temperature. *Agric and For Meteorol.* v.31, 159–166, 1984.

BROOKS, C.F.; BROOKS, E.S. Sunshine recorders: a comparative study of the burning glass and thermometric systems. *J. Meteorol.* v.4, 105-115, 1947.

BURIOL, G.A.; ESTEFAREL, V.; HELDWEIN, A.B.; PRESTE, S.D.; HORN, J.F.C. Estimativa da radiação solar global a partir dos dados de insolação, para Santa Maria – RS. *Ciência Rural*. v.42(9), 2012.

CAMPELO JUNIOR, J.I. Relação sazonal entre radiação solar global e insolação no sudoeste da Amazônia. *Rev Bras de Agromet*. v.6(2), 193-199, 1998.

CARVALHO, L.M.V.; JONES, C. Zona de Convergência do Atlântico Sul. In: CAVALCANTI, I.F.A.; FERREIRA, N.J.; SILVA, M.G.J.; SILVA DIAS, M.A.F (Org.). *Tempo e Clima no Brasil*. 1ed. 2009, São Paulo: oficina de textos, 1, pp 96-109

CHEN R.; LU, S.; KANG, E.; YANG, J.; JI, X. Estimating daily global radiation using two types of revised models in China. *Ener Conv and Manag* v.47, 865–878, 2006.

CONAB (2014) Companhia Nacional de Abastecimento. Indicadores da Agropecuária, setembro 2014. Brasília, DF. Publishing. http://www.conab.gov.br/OlalaCMS/uploads/arquivos/14_09_18_16_28_16_20_14-09-setembro.pdf. Accessed 29 September 2014

CONAB (2016) Companhia Nacional de Abastecimento. Monitoramento agrícola – Cultivos de inverno (safra 2015) e de verão (safra 2015/2016), Brasília, DF. Publishing. http://www.conab.gov.br/OlalaCMS/uploads/arquivos/16_03_11_15_20_36_bol_etim_graos_marco_2016.pdf. Accessed 30 March 2016

DALLACORT, R.; FREITAS, P.S.L.; GONÇALVES, A.C.A.; REZENDE, R.; BERTONHA, A.; SILVA, F.F.; TRINTINALHA, M.A. Determinação dos coeficientes da equação de Angström para a região de Palotina, estado do Paraná. *Acta Scien Agron*. v.26(3), 329-336, 2004.

DEVORE, J.L. Probabilidade e estatística: para engenharia e ciências. Thomson Pioneira, São Paulo, SP, 2006.

DORNELAS, K.D.S.; SILVA, C.L.; OLIVEIRA, C.A.S. Coeficientes médios da equação de Angström-Prescott, radiação solar e evapotranspiração de referência em Brasília. *Pesq Agropec Bras*. v.41(8), 1213-1219, 2006.

DUZEN, H.; AYDIN, H. Sunshine-based estimation of global solar radiation on horizontal surface at Lake Van region (Turkey). *Energy Convers. Manag*. v.58, 35 – 46, 2012.

EFRON, B. TIBSHIRANI, R.J. An introduction to the bootstrap. Chapman & Hall, New York, 1993.

ESCOBAR, C.J.E. Padrões de circulação em superfície e em 500 hPa na América do Sul e eventos de anomalias positivas de precipitação no estado de Minas Gerais durante o mês de dezembro de 2011. *Rev Bras de Meteorol*. v.29(1), 105 – 124, 2014.

HAY, J.E. Calculation of monthly mean solar radiation for horizontal and inclined surfaces. *Sol Ener*. v.23, 301-307, 1979.

IBGE – Instituto Brasileiro de Geografia e Estatística (2015). Publishing: <<http://cidades.ibge.gov.br/xtras/perfil.php?lang=&codmun=510790&search=mato-grosso|sinop|infograficos:-informacoes-completas>>. Accessed 23 July 2015.

LI, M.F.; TANG, X.P.; WU, W.; LIU, H.B.; General models for estimating daily global solar radiation for different solar radiation zones in mainland China. *Energy Convers. Manag.* v.70, 139-148, 2013

LIU, D.L.; SCOTT, B.J. Estimation of solar radiation in Australia from rainfall and temperature observations. *Agric and For Meteorol.* v.106, 41–59, 2001.

MARENGO, J.A; NOBRE, C.A. Clima da Região Amazônica In: Cavalcanti IFA, Ferreira NJ, Silva MGAJ, Dias MAFS (ed). *Tempo e Clima no Brasil*. São Paulo: Oficina de Textos, pp 197-212, 2009.

MEHARRAR, K; BACHARI, N.E.I. Modelling of radiative transfer of natural surfaces in the solar radiation spectrum: development of a satellite data simulator (SDDS), *Int. j. remote Sens.* v. 35(4), 1199 – 1216, 2014. DOI:10.1080/01431161.2013.876116

MENEZES, H.E.A.; DANTAS, R.T. Ajuste de funções para estimativa da Irradiação solar difusa em Cajazeiras – PB. In: XII Congresso Brasileiro de Meteorologia Foz do Iguaçu – PR, 2002.

PRESCOTT, J.A. Evaporation from Water Surface in Relation to Solar Radiation. *Transactions of the Royal Society of South Australia.* v.64, 114-118, 1940.

QUEIROZ, M.R.; NOGUEIRA, C.C.B.R.; ASSIS, S.V. Avaliação de um método empírico para estimativa da radiação solar global - modelo de Bristow-Campbell. In: Congresso Brasileiro de Meteorologia, 11, Rio de Janeiro (RJ), 2000. *Anais do XI Congresso Brasileiro de Meteorologia*, 2000, p. 194-199, 2000.

QUERINO, C.A.S.; MOURA, M.A.L.; LYRA, R.F.F.; MARIANO, G.L.M. Avaliação e comparação de radiação solar global e albedo com ângulo zenital na região Amazônica. *Rev. Bras. Meteorol.* v.21(3a), 42–49, 2006.

QUERINO, C.A.S.; MOURA, M.A.L.; QUERINO, J.K.A.S; VON RADOW C.; MARQUES FILHO, A.O. Estudo da radiação solar global e do índice de transmissividade (Kt), externo e interno, em uma floresta de mangue em Alagoas-Brasil. *Rev Bras de Meteorol.* 26(2): 204-294, 2011.

RENSHENG, C.; ERSI, K.; JIANPING, Y. SHIHUA, Z.W.; YONGJIAN, D. Estimation of Horizontal diffuse solar radiation with measured daily data in China. *Ren Ener.* v.29, 717 – 726, 2004.

RIVINGTON, M.; BELLOCCHI, G.; MATTHEWS, K.B.; BUCHAN, K. Evaluation of three model estimations of solar radiation at 24 UK stations. *Agric and For Meteorol.* v.132, 228–243, 2005.

SHEIL, D.M.D. How forests attract rain: an examination of a new hypothesis. *BioScie.* v.59(4), 341-347, 2009.

SOUZA, J.L.; NICÁCIO, R.M.; MOURA, M.A.L. Global solar radiation measurements in Maceió, Brazil. *Ren Ener.* v.30, 1203 – 1220, 2005.

THORNTON, P.E.; RUNNING, S.W. An improved algorithm for estimating incident daily solar radiation from measurements of temperature, humidity and precipitation. *Agric and For Meteorol.* v.93(4), 211-228, 1999.

TRNKA, M.; ZALUD, Z; EITZINGER, J.; DUBROVSKY, M. Global solar radiation in Central European lowlands estimated by various empirical formulae. *Agric and For Meteorol.* v.131(1–2), 54–76, 2005.

VIANELLO, R.L.; MAIA, L.P.G. Estudo preliminar da climatologia dinâmica do Estado de Minas Gerais. Revista Informe Agropecuário. v.12(138), 6-8, 1986.

WEISS, A.; HAYS, C.J.; HU, Q., EASTERLING, W.E. Incorporating bias error in calculating solar Irradiance: implications for crop simulations. Agron Jour. v.93(6), 1321-1326, 2001.

WILLMOTT, C.J.; ACKLESON, S.G.; DAVIS, J.J.; FEDDEMA, K.; KLINK, D.R. Statistics for the evaluation and comparison of models. Journal of Geophysical Research. v.90(5), 8995-9005, 1985.

YANG, K.; KOIKE, T. Estimating surface solar radiation from upper-air humidity. Sol Ener. v.72(2): 177-86, 2002